Engineering a highly elastic human protein–based sealant for surgical applications

Nasim Annabi[1,2,3,4,*], **Yi-Nan Zhang**[2,3,†], **Alexander Assmann**[2,3,4,5], **Ehsan Shirzaei Sani**[1], **George Cheng**[6], **Antonio D. Lassaletta**[6], **Andrea Vegh**[2,3], **Bijan Dehghani**[2,3], **Guillermo U. Ruiz-Esparza**[2,3], **Xichi Wang**[2,3], **Sidhu Gangadharan**[6], **Anthony S. Weiss**[7,8,9], **Ali Khademhosseini**[2,3,4,10,*]

[1]Department of Chemical Engineering, Northeastern University, Boston, MA 02115-5000, USA.

[2]Biomaterials Innovation Research Center, Brigham and Women's Hospital, Harvard Medical School, Boston, MA 02139, USA.

[3]Harvard-MIT Division of Health Sciences and Technology, Massachusetts Institute of Technology, Cambridge, MA 02139, USA.

[4]Wyss Institute for Biologically Inspired Engineering, Harvard University, Boston, MA 02115, USA.

[5]Department of Cardiovascular Surgery and Research Group for Experimental Surgery, Heinrich Heine University, Medical Faculty, Duesseldorf 40225, Germany.

[6]Division of Thoracic Surgery and Interventional Pulmonology, Beth Israel Deaconess Medical Center, Boston, MA 02215, USA.

[7]School of Life and Environmental Sciences, University of Sydney, Sydney, New South Wales 2006, Australia.

[8]Charles Perkins Centre, University of Sydney, Sydney, New South Wales 2006, Australia.

[9]Bosch Institute, University of Sydney, Sydney, New South Wales 2006, Australia.

[10]Department of Physics, King Abdulaziz University, Jeddah 21569, Saudi Arabia.

Abstract

Surgical sealants have been used for sealing or reconnecting ruptured tissues but often have low adhesion, inappropriate mechanical strength, cytotoxicity concerns, and poor performance in biological environments. To address these challenges, we engineered a biocompatible and highly elastic hydrogel sealant with tunable adhesion properties by photocrosslinking the recombinant

[*]Corresponding author. n.annabi@neu.edu (N.A.); alik@bwh.harvard.edu (A.K.).
[†]Present address: Institute of Biomaterials and Biomedical Engineering, University of Toronto, Toronto, ON M5S 3G9, Canada.

human protein tropoelastin. The subcutaneous implantation of the methacryloyl-substituted tropoelastin (MeTro) sealant in rodents demonstrated low toxicity and controlled degradation. All animals survived surgical procedures with adequate blood circulation by using MeTro in an incisional model of artery sealing in rats, and animals showed normal breathing and lung function in a model of surgically induced rat lung leakage. In vivo experiments in a porcine model demonstrated complete sealing of severely leaking lung tissue in the absence of sutures or staples, with no clinical or sonographic signs of pneumothorax during 14 days of follow-up. The engineered MeTro sealant has high potential for clinical applications because of superior adhesion and mechanical properties compared to commercially available sealants, as well as opportunity for further optimization of the degradation rate to fit desired surgical applications on different tissues.

INTRODUCTION

Sutures and staples have been widely used to reconnect incisions for recovering tissue structure and function. They hold tissues in close proximity to facilitate healing and resist applied mechanical loads. Although they are commonly used after surgery, these methods are not sufficient for many clinical applications, especially to prevent the leaking of liquids from incisions (1). Sealing wound tissue using sutures and staples can also be challenging and time-consuming and may not be possible in regions of the body that are not readily accessible (2). In addition, piercing tissues to place sutures and staples can further damage the surrounding wound area and can increasethe risk forinfection (1,3,4). Sealant materials have attracted attention as alternatives to seal and reconnect tissues or incorporate implant devices into tissues because of their ease of application and versatility (3, 5–7). Surgical sealants combined with sutures have been reported to more effectively seal wounds than sutures alone and provide a reduced infection rate and patient blood loss (3, 8, 9). To successfully develop sealants for the clinical practice, materials must provide adequate mechanical and adhesive properties for sealing the incision site without limiting tissue function or movement or causing adverse effects (1). In addition, to avoid the introduction of multiple foreign materials in the recipient and additional lesions caused by sutures and staples, it would be desirable to develop sealants that work effectively on elastic and fragile tissues without requiring the previous application of sutures or staples. For example, surgical glues for lung sealing should have a burst pressure higher than the maximum pressures exerted on the lung during physiological breathing (~1 to 2 mmHg) (10). In addition, an ideal lung sealant should be highly elastic (with an extensibility of up to 40%) and have an elastic modulus in the range of 5 to 30 kPa to support the lung tissue inflation and deflation (11, 12). On the other hand, suitable sealant for vascular sealing should exceed normal physiological blood pressures (up to 140 mmHg) and hypertensive peak values (rarely up to 300 mmHg) (13).

In lung surgery, prolonged air leakage is the most common complication after surgical dissection and resection (14, 15). Prolonged air leaks lead to extended chest tube drainage time, which can be associated with pain and immobilization, increased risk for developing infections and bronchopleural fistulae, longer hospital stays, and higher health care costs (16–19). Sealants have been used as connecting materials to close the incision and limit the duration of postoperative air leakage (1, 3). Various types of synthetic and naturally

derived materials, including fibrin- and collagen-based materials, have been tested to overcome these challenges (20). However, these surgical products cannot completely achieve the required adhesive and cohesive properties for lung incision sealing, such as tensile strength, elasticity, adhesive strength, and burst pressure resistance (20–24). Cyanoacrylate and gelatin-resorcinol-formaldehyde/glutaraldehyde glues have a much stronger adhesive strength to tissue, but their toxic degraded products prevent clinical translation (4, 23). Their nondegradable polymer nature can also cause tissue irritation and infection (23). FocalSeal is a nontoxic, nonimmunogenic, and bioabsorbable polyethylene glycol (PEG)– based synthetic hydrogel, which can be photopolymerized by blue-green light and has been approved by the U.S. Food and Drug Administration (FDA)for air leakage sealing after lung surgery (25,26).The clinical result showed that 77% of patients treated with FocalSeal had no postoperative air leak, compared to 9% of control group (26). However, the photochemical polymerization had three-step delivery requiring application of a primer layer followed by a PEG-based adhesive material and subsequent light exposure (26–28). Therefore, engineering a single-component sealant, which does not need a primer for better adhesion, might be more suitable for thoracic surgery. Another FDA-approved pleural air leak sealant is Progel, which is based on human serum albumin and a PEG crosslinker (29, 30). Progel has been introduced to the market to be used in lung procedures only in conjunction with sutures for better sealing. Trials with pulmonary resection patients showed that Progelapplicationinconjunctionwithsuturingandstaplingwassuperior to the use of suturing and stapling only. However, the high cost of human-based albumin and the potential for disease transmission, due to the fact that it is a blood-derived product, are the concerns with Progel. Another limitation of Progel is that it lacks a prohemostatic function, which may cause additional problems when applying the sealant to bleeding wounds. As a result of this, only 35% of patients treated with Progel after pulmonary resection were found to be air leak–free (29). In a recent study, Lang *et al.* developed a hydrophobic and elastic light-activated tissue adhesive for cardiovascular surgery (31). This highly elastic glue was formed by photocrosslinking of poly(glycerol sebacate acrylate) in the presence of a photoinitiator and ultraviolet (UV) light. The engineered glue could close the defects in a pig carotid artery with no bleeding after 24 hours of implantation. Because this material is made from a synthetic polymer in a process that uses organic solvent, there is an opportunity to make a water soluble and elastic naturally derived surgical sealant. Due to the limitations of the previously mentioned clinically available products, there is an unmet need to produce a new and more effective surgical sealant capable of sealing wounds in wet and dynamic biological environments while maintaining adequate mechanical and adhesion properties as well as promoting a time frame for tissue repair.

Here, we introduce an elastic hydrogel-based sealant with controlled mechanical and biodegradation properties using a modified recombinant protein, methacryloyl-substituted tropoelastin (MeTro). During surgery, this sealant can be applied over the defect site and rapidly photopolymerized to adhere strongly to soft tissues to stop air and liquid leakages, as well as to provide a time frame for tissue repair.

RESULTS

We formed a highly elastic and adhesive hydrogel using a light-cured recombinant protein, MeTro prepolymer. We have previously shown that the MeTro gel is an excellent candidate for skin, heart, and blood vessel tissue regeneration (32–35). The presence of various cell-binding sites in tropoelastin molecules promotes cellular adhesion and growth (36–38). In addition, the elastic properties of MeTro, with an extensibility of more than 400%, make it a suitable biomaterial for engineering elastic tissues. Here, we optimized the MeTro formulation to generate a highly elastic material that can be used as a surgical sealant for the sealing and repair of elastic tissues such as lungs and blood vessels. We produced a MeTro hydrogel with tunable mechanical and adhesive properties to select the hydrogel formulation with optimized mechanical stiffness, elasticity, burst pressure, and tissue adhesion based on the final application.

MeTro synthesis and its physical characterization

The MeTro prepolymer was synthesized using recombinant human tropoelastin and methacrylic anhydride (32). Physical properties of the hydrogel were tuned by controlling the degrees of methacryloyl substitution calculated by using ^{1}H nuclear magnetic resonance (NMR) analysis (fig. S1). MeTro prepolymers with 54% (low), 76% (medium), and 82% (high) degrees of methacryloyl substitution were synthesized using 8, 15, and 20% (v/v) of methacrylic anhydride, respectively. MeTro hydrogels were then formed through photocrosslinking of prepolymers with a UV light (6.9 mW/cm^2; 360 to 480 nm) at different exposure times ranging from 30 to 180 s. A photoinitiator [2-hydroxy1-(4-(hydroxyethoxy)phenyl)-2-methyl-1-propanone (Irgacure 2959); 0.5%, w/v] was used to form hydrogels.

The mechanical properties of MeTro gels at varying prepolymer concentrations and degrees of methacryloyl substitution were characterized by performing tensile and cyclic compression tests. The detailed experimental procedures are presented in the Supplementary Materials. Tensile tests on MeTro hydrogels showed that the elastic modulus and ultimate tensile strength of engineered hydrogels could be tuned by varying MeTro concentrations (Fig. 1A) and degrees of methacryloyl substitution (fig. S2). The fabricated MeTro gels showed elastic moduli of 16.5 ± 3.0 kPa, 27.8 ± 4.9 kPa, and 49.8 ± 4.0 kPa [$P < 0.01$ between 5 and 10% (w/v), $P < 0.0001$ between 10 and 20% (w/v), and $P < 0.0001$ between 5 and 20% (w/v)]. The ultimate tensile strengths of MeTro gels with medium degree of methacryloyl substitution were determined as 21.7 ± 5.5 kPa, 44.8 ± 8.2 kPa, and 52.6 ± 5.2 kPa for MeTro concentrations of 5, 10, and 20% (w/v), respectively (Fig. 1A). The increase in the elastic modulus of the engineered hydrogels may be due to the increased crosslinking density at a higher MeTro concentration. Although the elastic modulus of Progel, the FDA-approved surgical lung sealant, is higher than MeTro, both the tensile strength (42.1 ± 3.2 kPa) and elongation (25 ± 2%) of Progel were significantly lower than MeTro ($P < 0.05$) (fig. S3). In a recent study, a highly elastic photocrosslinked gelatin-based sealant has been developed (38, 39). Although the engineered sealant exhibited an elongation of up to 650%, the relatively low stiffness (~14 kPa) makes it unsuitable for the sealing of highly stressed tissues such as lungs and arteries. The high elasticity and tensile strength of the MeTro

hydrogel show its potential for sealing and repair of elastic tissues such as lung, cardiac tissues, or blood vessels (32, 33, 41).

Cyclic compression testing on MeTro hydrogels with varying protein concentrations and degrees of methacryloyl substitution showed high resilience of the engineered hydrogels (Fig. 1B and fig. S4). The compressive moduli of MeTro with medium methacryloyl substitution enhanced from31.8± 3.6 kPa to57.6 ± 10.9 kPa and 167.1 ±32.2 kPa by increasing the MeTro concentration (Fig. 1B, i and ii). These results follow the trends set from tensile testing shown in Fig. 1A. The energy loss for cycle 20 was found to be 36.6 ± 1.8%, 34.0 ± 0.7%, and 36.4 ± 0.1% for 5, 10, and 20% (w/v) MeTro gels, respectively (Fig. 1B, iii).

The porosity and swelling properties of a hydrogel play a major role in new tissue generation (42). The MeTro hydrogel's porosity and swelling behavior were influenced by the MeTro concentration (Fig. 1, C and D). We compared the structure of freeze-dried samples by using scanning electron microscopy (SEM) analysis. Although lyophilization can generate some pores in hydrogels, we observed a decrease in pore sizes by increasing the MeTro concentration for the samples that were prepared and freeze-dried using the same conditions (freezing temperature and duration) for lyophilization (Fig. 1C). After 12 hours, the swelling ratios achieved the maximum values of 208.0 ± 30.0%, 168.3 ± 22.4%, and 114.9 ± 31.1% for hydrogels produced by using 10, 15, and 20% (w/v) MeTro concentrations, respectively (Fig. 1D). Although the pores observed in SEM images of lyophilized hydrogels may be artifacts, the reduced swelling ratio in hydrogels produced at higher MeTro concentrations may be relevant to the molecular weight between crosslinks (43). The reduced swelling ratio for hydrogel with higher MeTro concentration can be beneficial for sealant applications because of their minimal deformation and stronger interaction with the native tissues.

In vitro adhesion testing on MeTro hydrogels: Lap shear, burst pressure, and wound closure tests

Various ASTM (American Society for Testing and Materials) standard tests were performed to evaluate the in vitro sealing properties of the MeTro hydrogel. Standard lap shear, burst pressure, and wound closure tests were performed on MeTro sealants produced by varying protein concentrations and degrees of methacryloyl substitution, as well as several commercially available sealants including a fibrin-based sealant (Evicel), a PEG–based sealant (Coseal), and a human serum albumin/PEG–based sealant (Progel).

Lap shear testing was used to determine the shear strength of the sealant based on the ASTM F2255–05 standard (Fig. 2A, i) using two pieces of glass slides coated with gelatin solution as substrate. The lap shear strength of the MeTro sealant with the medium methacryloyl substitution increased from 31.0 ± 3.9 kPa to 42.1 ± 6.3 kPa and 81.3 ± 12.7 kPa with increasing MeTro concentrations [$P < 0.0001$ between 5 and 20% (w/v)] (Fig. 2A, ii and iii). The highest shear strength (172.1 ± 21.7 kPa) was achieved by using a 20% (w/v) MeTro gel with high methacryloyl substitution, which was comparable to the shear strength value obtained for Progel (184.1 ± 40.5 kPa) and significantly higher than those for Evicel (69.6 ± 17.7 kPa) and Coseal (69.7 ± 20.6 kPa) ($P < 0.0001$) (Fig. 2A, iii). The failure in the lap

shear test was likely due to the cohesion failure of the MeTro hydrogels because the residual ofMeTro sealants was observed on gelatin-coated slides after the test. In addition, the strain at break for the MeTro sealant was much higher than that for Progel (Fig. 2A, ii).

In vitro burst pressure testing based on the ASTM F2392–04 standard was performed using wet collagen sheet as substrate to determine the ability of the engineered materials to seal tissues under airorliquidpressures(Fig.2B,i).Theburst pressure of the MeTro sealantwith medium methacryloyl substitution increased from 0.12 ± 0.02 kPa to 4.9 ± 0.1 kPa and 9.2 ± 2.1 kPa with increasing MeTro concentrations from 5% to 10 and 20% (w/v), respectively ($P < 0.01$) (Fig. 2B, ii and iii). The burst pressure of the engineered MeTro sealant reached a maximum value of 11.9 ± 1.5 kPa byusing 20%(w/v) MeTro with high methacryloyl substitution (Fig. 2B, iii). Sealants made of 20% (w/v) MeTro prepolymer with medium and high methacryloyl substitution showed a much higher in vitro burst pressure than Evicel (3.2 ± 1.3 kPa), Coseal (1.7 ± 0.1 kPa), or Progel (4.3 ± 0.7 kPa) ($P < 0.0001$), pointing to the high burst pressure resistance of the MeTro gel and supporting its suitability as a sealant material for use in dilating tissues. This property is particularly beneficial for use as a lung sealant because proper sealing of lung tissues requires materials that can withstand the high pressures occasionally exerted on pulmonary tissue during invasive mechanical ventilation, for example, by recruitment maneuvers. In this scenario, pressure values can reach up to 40 cmH_2O of intra-alveolar peak pressure (3.9 kPa) (44).

Wound closure tests were performed to determine the adhesive strength of the engineered sealants on native tissue (porcine skin) according to the ASTM F2458–05 standard (Fig. 2C, i). The adhesive strength of the MeTro sealant with medium methacryloyl substitution increased from 18.6 ± 5.1 kPa to 31.5 ± 6.5 kPa and 53.8 ± 8.9 kPa by increasing the MeTro concentration from 5% to 10 and 20% (w/v), respectively ($P < 0.0001$) (Fig. 2C, ii and iii). The highest adhesive strength (75.9 ± 7.7 kPa) was obtained for the sealant produced by using 20% (w/v) MeTro prepolymer with high methacryloyl substitution (Fig. 2C, iii). This value was significantly higher than the adhesive strength of Evicel (20.8 ± 6.7 kPa) and Coseal (26.3 ± 4.7 kPa) ($P < 0.0001$). The elongation of the MeTro gel (120%) in the wound closure test was twofold higher than Progel (55%), confirming the previous finding that the MeTro gel displays a higher elasticity than Progel. Overall, the unique combination of in vitro sealing properties of the MeTro gel with 20% MeTro concentration and high degree of methacryloyl substitution offers substantial advantages over the commercially available products for wound tissue sealing, particularly due to its superior elasticity, adhesive strength, and burst pressure resistance.

In vitro cytocompatibility of the MeTro sealant

The engineered MeTro hydrogels could support the growth and proliferation of mesenchymal stem cells (MSCs) and endothelial progenitor cells (EPCs) as model cells, confirming the in vitro cytocompatibility of the sealant. Both cell types were cultured on the surface of the MeTro hydrogel for 7 days. Cell viability and activity were studied for each cell type (MSCs or EPCs), as well as for a coculture of both cell types (MSCs and EPCs) (fig. S5). Cell viability was higher than 95% over 7 days for MeTro gels seeded with MSC and EPC monocultures or coculture of MSCs/EPCs, suggesting that the MeTro

gel is not cytotoxic (fig. S5, A to C and J). The cells had adhered to the hydrogel, as identified by the F-actin cell filaments and 4′,6-diamidino-2-phenylindole (DAPI) nuclei staining (fig. S5D). By day 7 of culture, a confluent layer of MSCs was formed on the MeTro hydrogel (fig. S5G). In addition, immunostaining on EPC-seeded scaffolds on days 3 and 7 of culture indicated the expression of CD31 markers, confirming the differentiation of EPCs to endothelial cells on the MeTro gel, which was increased from day 3 to day 7 (fig. S5, E and H). Moreover, immunostaining for a-smooth muscle actin (α-SMA) and CD31 on MSC/EPC-seeded MeTro hydrogels confirmed the differentiation of EPCs to endothelial cells and the differentiation and activation of MSCs toward a contractile phenotype after 3 days (fig. S5F). By day 7 of culture, a confluent layer of MSCs/EPCs had formed on the MeTro gel (fig. S5I). The metabolic activity of the cells was quantified by a PrestoBlue assay, which showed a significant increased in relative fluorescence intensity from day 1 to day 7 ($P < 0.0001$), suggesting that cell proliferation and activity increased on the MeTro gel (fig. S5K). These results collectively demonstrate the capacity of the MeTro gel to serve as a biocompatible sealant material that promotes cell adhesion, growth, and proliferation.

In vivo biodegradation and biocompatibility of MeTro gels

The in vivo degradation of MeTro gels produced by using various MeTro concentrations and degrees of methacryloyl substitution was evaluated after subcutaneous implantation into rats (Fig. 3A). Samples were explanted on days 7, 28, and 84 to measure their weights and sizes. Macroscopic views of the MeTro hydrogels before implantation and after explantation on days 7, 28, and 84 are shown in Fig. 3A (i). In vivo degradation rates were quantified by measuring sample volumes (Fig. 3A, ii and iv) and weights (Fig. 3A, iii and v) on days 0, 7, 28, and 84 after implantation. As shown in Fig. 3A, hydrogels produced by using lower MeTroconcentrationsandmediummethacryloylsubstitutiondegraded faster, with respect to both volume and weight, compared to MeTro hydrogels with higher protein concentration. However, there were no methacryloyl substitution degree–dependent differences in the time course of the volume and dry weight changes for 10% (w/v) MeTro hydrogels (Fig. 3A, iv and v). Although all hydrogel conditions resulted in progressive degradation, 100% degradation was reached only in the 5% (w/v) group by day 84. Controlling the degradation rate of the sealant is critical to ensure that the sealant material does not completely degrade before tissue healing (3, 45).

Hematoxylin and eosin (H&E) staining revealed a small amount of mononuclear inflammatory cell recruitment, indicating a minor local host inflammatory response (Fig. 3B). At day 28, cellular infiltration was slightly pronounced; however, it still occurred in the normal host response range (Fig. 3B, ii). Furthermore, the histologically assessed tissue architecture at day 28 resembled a thin fibrous capsule around the implants, implying collagen formation in an inflammatory context. Thus, fluorescent immunohistological staining for macrophages (CD68) and lymphocytes (CD3) was used to further characterize the local immune response. CD68^{+} macrophage invasion at the interface between the MeTro gel and the subcutaneous tissue was observed at day 3 but not at days 28 and 84 (Fig. 3C, i to iii). We also did not detect CD3^{+} lymphocyte infiltration at any time point (Fig. 3C, iv to vi). These results demonstrated that subcutaneously implanted MeTro sealants evoked minimal inflammatory responses by the host organism.

Ex vivo and in vivo sealant performance using small- and large-animal models

To investigate the potential of MeTro material to seal defects in elastic tissues, in vivo and ex vivo experiments were performed on rat arteries, rat lungs, and porcine lungs. Optimized MeTro formulations with 10 and 20% (w/v) MeTro concentrations and high methacryloyl substitution were used for the ex vivo and in vivo experiments. Because of the high burst pressure, preferable tissue adhesion, and mechanical properties of MeTro noted during in vitro tests, the in vivo experiments were performed using MeTro as the sealant material alone, without the use of sutures.

Ex vivo (Fig. 4A) and in vivo (Fig. 4, B to D, and fig. S6) rat artery incision models were used to test the sealing properties of MeTro in the presence of extensive bleeding. The MeTro sealant was used to seal the anastomosis points created in an explanted rat abdominal aorta (Fig. 4A, i). In an ex vivo experiment, the aorta was sliced into pieces with a length of 4 cm. MeTro gels were then either directly applied to the anastomosis points of the aorta or made as a patch and then applied to the two ends of the aorta tube segments. The adhesive strength of the MeTro sealant applied on one side or both sides of the aorta was compared to that of Evicel. The MeTro gel applied to both sides of the aorta significantly increased the adhesive strength from 64.1 ± 6.0 kPa to 99.0 ± 17.7 kPa compared to the single-side sealing ($P < 0.05$). The adhesion strength of the MeTro gel in both types of conditions (applied single-sided and double-sided) was significantly higher than that of Evicel applied to one side (23.6 ± 8.0 kPa; $P < 0.01$) or both sides (41.1 ± 10.1 kPa; $P < 0.001$) of the tissue (Fig. 4A, iii). A MeTro hydrogel patch was generated, wrapped around the two artery tube segments, and sealed by applying the MeTro prepolymer solution and photocrosslinking (Fig. 4A, ii). In this setting, a much higher adhesive strength (162.3 ± 25.0 kPa) ($P < 0.001$) was achieved when compared to applying the MeTro sealant only (Fig. 4A, iii). This patch may be used to bridge arterial wall substance defects while maintaining the elastic properties of the vascular wall. The adhesive strength of MeTro (162.3 kPa or 1217 mmHg) exceeds normal physiological blood pressures (up to 140 mmHg), as well as hypertensive peak values (rarely up to 300 mmHg) (13).

The in vivo experiments using a rat artery incision model in the abdominal aorta demonstrated that the MeTro gel sealed the otherwise lethal incision effectively and achieved hemostasis (Fig. 4B, i and ii). After surgery, the rats presented an adequate perfusion of the lower limbs located downstream of the defect site. All animals survived the follow-up time. Artery burst pressure tests were conducted on day 4 after surgery. These burst pressure experiments revealed that the arteries did not burst from regions where the MeTro was applied but rather from other areas, confirming that the sealing was effective (Fig. 4B, iii). The burst pressure values of MeTro-sealed arteries (95.5 ± 8.8 kPa) were similar to those of healthy arteries at day 4 (94.4 ± 15.3 kPa) (Fig. 4B, iv).

The microstructure and coherence of the adhesive interfaces between the MeTro sealant and the native artery were studied by SEM and histology analyses (Fig. 4, C and D). The magnified microstructure showed obvious tight interfaces between the MeTro hydrogel and the artery. This coherent adhesive interface indicated a strong bond between the sealant and the tissue. This was further confirmed by light microscopy after H&E staining, as shown in Fig. 4D (between MeTro and artery). Because MeTro was applied as a prepolymer solution,

it was able to penetrate into the tissue interface. After photocrosslinking, the MeTro gel remained entangled within tissue fibers. The phenomenon that adhesive material and tissue collagen fibers tend to interlock at interfaces has been previously reported by Lang *et al.* (31). In addition to this physical interaction and interlocking, charge interactions (positively charged tropoelastin and negatively charged glycosaminoglycans) can further improve the adhesion of MeTro to the tissues (46).

A rat lung incision model was used to study the in vivo sealing properties of MeTro sealant produced by using 20% (w/v) MeTro concentration at high methacryloyl substitution (Fig. 5A and fig. S7). Four days after surgery, the sealed lung tissues were explanted and burst pressures were measured to compare with day 0. The burst pressure of the MeTro sealant was also compared with those of Evicel, Progel, and suturing controls on day 0. The typical mode of failure for MeTro-sealed tissue on day 0 was not the bursting of the material but rather of native lung tissue outside of the defect area (Fig. 5A, i and ii, and movie S1). In contrast, Evicel and Progel failed by direct material bursting at 2.7 ± 0.7 kPa and 2.2 ± 0.7 kPa, respectively, which was due to the low mechanical properties of the adhesives (Fig. 5A, iii). For incisions closed by sutures, the lung tissue burst around the suture points at 3.1 ± 0.7 kPa on day 0. The burst pressure of the MeTro sealant immediately after curing on the lung tissue (day0) was6.2 ± 0.7 kPa,which was significantly higher than those of Evicel, Progel, and suture-only closures ($P < 0.0001$) (Fig. 5A, iii). Extensive air leakages from the lung tissue sealed by Evicel or sutures lead to lethal pneumothorax shortly after extubation. Therefore, chronic survival tests were continued using 20% MeTro sealant alone for up to 1 month. Four days after surgery, the burst pressure of MeTro-sealed lung tissue was equal to that of native healthy rat lung tissue (6.4 ± 0.5 kPa versus 6.8 ± 0.8 kPa) (Fig. 5A, iii). In addition, SEM and histology analyses showed tight interfaces between the MeTro hydrogel and the lung tissues, indicating strong bonding and interlocking at the interfaces (Fig. 5, B and C).

We performed H&E staining (Fig. 5D) and immunohistological analysis (Fig. 5E) to evaluate the interaction between the MeTro sealant and the tissue after 7 and 28 days. H&E staining from sealant/tissue interface showed that MeTro remained attached to the tissue on both day 7 (Fig. 5D, i) and day 28 (Fig. 5D, ii) with no marked changes in the morphology of the sealant, confirming that the sealant remained intact over 1 month with no or little degradation. In addition, no apparent signs of fibrous capsule formation were observed around the sealant material. To study the effects of increasing the in vivo degradation rate, we incorporated matrix metalloproteinase–2 (MMP-2) into the MeTro prepolymer before crosslinking. It has been reported that MMP enzymes digest specific proteins in extracellular matrix (ECM), especially elastic fibers made of tropoelastin (47, 48). MMP-2 is mainly expressed during embryonic development and is considered a catalyst for ECM degradation (49). Before invivo experiments, weperformed in vitro degradation testing using the MeTro hydrogel loaded with different concentrations of MMP-2 (0, 0.1, 1, and 10 μg/ml) to optimize MeTro-MMP formulations. Maximum degradation was achieved after 20 days of incubation in phosphate-buffered saline (PBS) for the samples containing MMP-2 (10 μg/ml) (fig. S8). Next, we incorporated MMP-2 (10 μg/ml) in 20% MeTro prepolymer solution and photopolymerized it on rat lung tissues using the in vivo incisional model. H&E staining from the interface of lung tissue and MeTro-MMP sealant showed that the MeTro-

MMP samples showed a pitted structure with many cavities at day 7, which could be due to degradation of the MeTro hydrogel in the presence of MMP-2 (Fig. 5D, iii). At day 28, the MeTro-MMP samples(Fig. 5D,iv)showedalooserstructureascomparedtotheMeTro sealant (Fig. 5D, ii), confirming the enzymatic degradation of the MeTro-MMP samples after 1 month in vivo. The immunofluorescent staining of the MeTro and MeTro-MMP samples exhibited negligible leukocyte infiltration, as demonstrated byminimal CD3 expression on both days 7 and 28 (Fig. 5E). In contrast, macrophage infiltration (CD68 antigen) was observed at day 7 for both samples (Fig. 5E, i and iii). However, the expression of CD68 was reduced after 28 days for the MeTro samples (Fig. 5E, ii), but the amount of macrophages remains the same for the MeTro-MMP samples at day 28 (Fig. 5E, iv).

Ex vivo and in vivo sealant tests on porcine lungs

Encouraged by the sealing functionality of MeTro on rat lungs, we proceeded toward a model environment that better represented the human scenario. Explanted porcine lungs were first used to investigate the adhesion properties of the MeTro sealant before in vivo tests. Defects were created on deflated porcine lungs and sealed by applying and photopolymerizing the MeTro prepolymer solution. The pig lung incision site before and after the sealing is shown in Fig. 6A (i and ii) and movieS2.A representative graph depicting the increase in pressure over time during burst pressure testing is illustrated in Fig. 6A (iii). The average burst pressures were determined as 2.92 ± 0.49 kPa, 1.43 ± 0.40 kPa, 1.90 ± 0.44 kPa, and 1.83 ± 0.51 kPa for 20% MeTro, Evicel, Progel, and surgical sutures only, respectively (Fig. 6A, iv). These results show that the MeTro sealant has a significantly greater sealing ability than the other clinically available sealant materials and sutures ($P < 0.01$ between MeTro and Evicel and $P < 0.05$ between MeTro and Progel or sutures).

Preclinical functional evaluation of the MeTro sealant was conducted in a porcine model of severe lung injury (fig. S9). After making a standardized pulmonary air and blood leak (Fig. 6B, i), MeTro prepolymer was applied and photopolymerized in vivo to seal the defect (Fig. 6B, ii). During a follow-up period of 14 days, no generation of pneumothorax, which would indicate air leakage, occurred as monitored by ultrasound imaging (Fig. 6B, iii and iv). Histology at day 14 revealed wound repair by dense fibrous tissue (Fig. 6B, v) predominantly containinga collagenous network and fibroblasts (Fig. 6B,vi).The sealant cover remained adherent to the defect site and the surrounding tissue (Fig. 6B, vii). Immunohistological analyses showed a minor presence of macrophages in the wound repair area around the sealant and no relevant infiltration with lymphocytes (Fig. 6B, viii). These data confirm our hypothesis that the highly elastic MeTro hydrogel is capable of sealing severe pulmonary air and blood leakage in the absence of additional staples or sutures in a preclinical large-animal model. Further experiments are warranted to evaluate the long-term fate of MeTro sealant implants.

DISCUSSION

To date, the most widely used surgical sealants are classified on the basis of their chemical compositions as follows: cyanoacrylate adhesives, synthetic polymer–based materials, and natural polymer–based materials (50–53). Although many clinical sealant materials are

commercially available, a need for the development of new sealants tailored to specific applications remains (table S1). Providing a strong tissue adhesion with minimized toxicity, host inflammation, and side effects is a major challenge (53). Recently, a highly elastic photocrosslinkable gelatin-based lung sealant, manufactured by dityrosine crosslinking supported by ruthenium and sodium persulfate (SPS), was developed (39). The final sealant formulation exhibited an extensibility of up to 650%; however, its low elastic modulus (14 kPa) indicates that the cohesive properties may not be suitable for use as a lung sealant. In vitro and in vivo studies in a sheep lung defect model revealed the toxicity of the material, attributed to ruthenium and the high concentrations of SPS (20 mM) and porcine gelatin (17.5%) that were necessary to generate these highly elastic gelatin hydrogels. The engineered gelatin sealant was not applied as a stand-alone therapy but rather required the use of sutures.

Another limitation of commercially available sealants is their low adhesive strength, particularly in the biological and dynamic environments (51, 52). Cyanoacrylate-based sealants exhibit high adhesive strength but are more rigid than native tissues and have a high cytotoxicity, contraindicating their internal use in the body (54–56). Fibrin-based sealants have characteristics similar to soft tissues but provide low adhesion, particularly to wet tissues (57, 58). In a recent study, Behrens *et al.* developed a novel sealant material based on poly(lactic-*co*-glycolic)/PEG for cecal intestinal anastomosis in combination with suture (58). The in vivo burst pressure testing showed that the combination of the engineered material with sutures had a burst pressure of about 70 mmHg (9.33 kPa), which was significantly higher than that of the control fibrin glue (20 mmHg or 2.67 kPa).

Currently, there is no commercially available elastic and biocompatible sealant that is commercialized to be used suture-less for wound closure. This is mainly due to the low elasticity (for example, Progel), low adhesion to wet tissues (such as fibrin-based sealants), and inappropriate mechanical strength (such as high stiffness in BioGlue and low mechanical properties in hydrogel-based sealants). Therefore, it is expected that the optimized MeTro formulation can overcome all these limitations and will be widely used as an elastic surgical material with tunable properties for sealing internal elastic tissues without sutures.

Here, we engineered a UV light–photocrosslinked, highly elastic, biocompatible, and slowly biodegradable sealant material using a modified human protein. The mechanical properties of the MeTro sealant provide higher tensile strength and elongation as compared to Progel. The MeTro hydrogel offers superior adhesive strength and burst pressure resistance as compared to commercially available clinical sealants (Evicel, Coseal, and Progel). The engineered MeTro gel offers a strong support to overcome liquid and air leakages resulting from surgical procedures without the need for suturing. First, the selected formulation was used to seal elastic tissues such as lungs and blood vessels in small-animal models of tissue injury. After that, we tested the engineered MeTro sealant in a large-animal model of lung leakage to confirm its sealing capacity and biofunctionality in an environment closer to that found in the human body. Our in vivo results suggest that the MeTro sealant has excellent sealing properties, biocompatibility, and biodegradability in terms of minimal inflammatory host responses with tunable degradation. The MeTro sealant can provide flexibility without

compromising adhesion to prevent fluid leakages in different surgical conditions, promoting stable defect fixation during a time frame that is required for tissue repair and regeneration. Many biomedical applications, such as tissue sealing during surgical procedures (32, 41), could benefit from the highly elastic, slowly degrading, biocompatible MeTro sealant. However, long-term in vivo studies are necessary to definitely rule out potential toxicity.

In addition, we have shown that the MeTro precursor can be easily delivered in vivo and photopolymerized to close incisions with any shapes and sizes without the need for suturing. The use of light for crosslinking allowed control over the polymerization rate and application of the sealant material. This can potentially overcome many limitations of commercially available two-mixture component sealants (such as Evicel and Progel) such as uncontrolled and fast polymerization rate upon mixing the two components. In some cases, the fast and uncontrolled polymerization of the sealant during application can block the applicator and the tip, which will be required to be exchanged several times. However, the engineered MeTro sealant can be delivered at the incision site and photopolymerized in situ in a controlled manner using a small optical fiber. In addition, as the MeTro prepolymer coacervates at body temperature due to the interaction between the hydrophobic domains in tropoelastin (60, 61), the prepolymer solution is physically crosslinked upon introduction at the incision site and further photopolymerized to form a highly stable and adhesive sealant. The coacervation of MeTro prepolymer before photocrosslinking increases the viscosity of the solution to confine the material on the incision site for better sealing. This is another advantage of our system versus other sealant materials where there is a risk of losing sealing materials before gelation. Our future work will focus on revealing a better understanding of other adhesion mechanism for the MeTro sealant to guide the next-generation formulation.

Overall, our in vitro and in vivo data suggest that the MeTro gel is superior to clinical sealants because of its unique physical and mechanical properties, as well as the interaction between the sealing materials and the wound tissue. We envision that this sealant has potential for commercialization and can be used for sealing elastic tissues without the need for suturing. Our future work will focus on long-term in vivo experiments to assess the complete degradation of MeTro hydrogels, their effect on tissue healing, and any consequential responses. Although the use of UV light did not induce tissue damage, in our future work, we will focus on engineering a variant of the MeTro-based adhesive, which can be crosslinked using visible light. Although the production cost of MeTro is much lower than Progel ($50/ml versus $225/ml), the development of lower-cost MeTro sealant formulations may be considered.

MATERIALS AND METHODS

Study design

The objective of this study was to engineer a photocrosslinked, elastic, biocompatible, and biodegradable sealing material using a modified human protein. This sealant should provide a strong support to overcome the liquid leakages after surgical procedures. We hypothesize that one of the advantages in using recombinant human tropoelastin is that the MeTro prepolymer solution coacervates at the incision site to increase the viscosity of the solution due to multiple hydrophobic domains in tropoelastin. The solution can be further

photopolymerized to form a highly stable and adhesive sealant. In vitro sealing properties of the MeTro sealant were tested using lap shear, burst pressure, and wound closure tests to optimize the protein concentration and degrees of methacryloyl substitution and compared it to the commercially available sealants. In vivo degradation and biocompatibility were assessed in a rat subcutaneous model. The potential of the MeTro hydrogel for sealing of elastic and soft tissues was tested in a rat artery incision model ($n = 5$) and a rat lung leakage model ($n = 5$). The ability of the MeTro sealant to seal incision in large animals was tested using a porcine model ($n = 3$) in the absence of sutures or staples. The clinical or sonographic signs of pneumothorax were followed up to 14 days. The in vivo biocompatibility of the MeTro gel was evaluated and analyzed by a blinded pathologist. Other data were not blinded. No data were excluded from this study. Individual subject-level data are shown in table S2.

Synthesis of MeTro prepolymer

MeTro was synthesized by adding varying methacrylate anhydride (MA; Sigma-Aldrich) volumes into a tropoelastin (Elastagen Pty Ltd.) solution in PBS. This reaction was performed at 4°C for 12 hours. The extent of methacryloyl substitution was increased by adding higher concentrations of MA [8, 15, and 20% (v/v)]. The solutions were diluted and dialyzed with distilled water (Slide-A-Lyzer MINI; molecular weight cutoff, 35,000; Thermo Fisher Scientific) at 4°C for 3 days to remove the excess MA and methacrylic acid by-product. After dialysis, the MeTro solutions were filtered through a 70-μm Nylon cell strainer (Corning Life Sciences). Solutions were stored in a freezer at −80°C for 24 hours and subsequently lyophilized. The final products were stored at 4°C devoid of any light.

Characterization of MeTro

^{1}H NMR analyses were performed to calculate the degree of methacryloyl substitution of MeTro prepolymer samples. ^{1}H NMR spectra were obtained for MeTro with varying degrees of methacryloyl at 4°C using a Varian Inova-500 NMR spectrometer. Peak values of ^{1}H NMR spectra between 5.3 and 6.5 ppm of methacryloyl-substituted groups were used to determine the methacryloyl substitution degree. The peak at 3ppmcorrelated withthepresence of lysineresidues intropoelastin.The degrees of methacryloyl substitution (54, 76, and 82%) of MeTro prepolymers were calculated by ^{1}H NMR analysis based on the volume of added MA[8, 15,and 20% (v/v)]duringthereaction. Various degreesof methacryloyl substitution are defined as low for 54%, medium for 76%, and high for 82% throughout the article.

Synthesis of the MeTro hydrogel

MeTro hydrogels were formed by using MeTro prepolymers with varying degree of methacryloyl substitutions (low, medium, and high) and MeTro concentrations [5, 10, and 20% (w/v)] in a 0.5% (w/v) photoinitiator (Irgacure 2959, Ciba Chemicals) solution in PBS at 4°C. Hydrogels were formed through photocrosslinking with UV light (6.9 mW/cm^2; 360 to 480 nm) for an exposure time of 30 s to 3 min depending on the thickness of the MeTro gels.

In vitro lap shear test

The shear resistance of the MeTro gel (n 4), Evicel (Ethicon; $n = 5$), Coseal (Baxter; $n = 3$), and Progel (Neomend; $n = 4$) was tested according to the modified ASTM F2255–05 standard for lap shear strength property of tissue adhesives. Two glass slides (10 mm × 50 mm) were used to hold each sample. The top portion of the glass slides (10 mm× 15 mm) was coated with gelatin solution that was dried at room temperature before adding the sealant samples. The MeTro prepolymer solution (20 μl) was added to one of the gelatin-coated regions, and then the other slide was carefully put on the MeTro solution. After assembly, the MeTro gel between the two gelatin-coated glass slides was photocrosslinked by UV light. The two glass slides were placed into an Instron mechanical tester for shear testing by tensile loading with a strain rate of 1 mm/min. The sealant shear strength was determined at the point of detaching.

In vitro burst pressure test

The burst pressures of the MeTro gel [n 4, except 5% Metro ($n = 2$)], Evicel ($n = 4$), Coseal ($n = 3$), and Progel ($n = 5$) were obtained by using the ASTM F2392–04 standard, which is a standard test method for sealant material burst pressure. Porcine collagen I sheets (Savenor'sMarket) were cut to a dimension of 40 mm × 40 mm and submerged into PBS at room temperature for 1 hour. The wet collagen sheet was placed between two Teflon plates (35 mm × 35 mm) (McMaster-Carr), in which the upper piece had a 10-mm-diameter hole in its center. A 3-mm-diameter defect was created by a dermal biopsy punch (Miltex) and to be filled with the sealant material in the center of collagen sheet. The MeTro solution (20 μl) was manually injected onto the defect on the collagen using a pipette and photocrosslinked by irradiation with UV light. The sealed collagen sheet was then placed into a custom-designed burst pressure apparatus, as shown in Fig. 2B (i). The measured data were directly recorded by a connected PC.

In vitro wound closure test

The wound closure of the MeTro sealant (n 4), Evicel ($n = 5$), Coseal ($n = 3$), and Progel ($n = 3$) was tested using the modified ASTM F2458–05 standard, which is a standard test for the determination of tissue/sealant material adhesive strength. Porcine skin and rat artery were prepared as impaired tissues. Fresh porcine skin pieces were obtained from a local slaughterhouse and further cut into smaller pieces. Aortic arteries were extracted from rats ($n = 10$). The sample dimensions were 15 mm × 5 mm in area for the porcine skin and 15 mm in length for the rat artery. Tissues were immersed in PBS before testing to prevent drying. The tissues were fixed onto two precut poly(methyl methacrylate) slides (20 mm × 60 mm) using an ethyl 2-cyanoacrylate glue (Krazy Glue). Spaces (6 and 3 mm) were kept between the slides due to the length of the porcine skin and rat artery, respectively. Petroleum jelly was added at both ends of the adhesive defining the desired area of coverage (6 mm × 5 mm for the porcine skin and 3 mm × 2 mm for the rat artery). The tissue was then separated in the middle with a straight edge razor to simulate wounding. MeTro solution was administered onto the desired adhesive area and crosslinked by UV light. The double-sided sealant test was performed by flipping the sample and injecting another 10 μl of the MeTro gel onto the other side of the artery to seal the anastomosis points. In addition, a MeTro

patch made from MeTro gels was wrapped in the middle of two pieces of the aorta using the MeTro gel (10 μl) to connect the two ends of MeTro patch with the aorta. Maximum adhesive strength of each sample was obtained at the point of tearing.

Animal experiments

The small-animal experiments were performed on male Wistar rats (200 to 250 g) purchased from Charles River Laboratories. All rat experiments were conducted in the Partners Research Building. Isoflurane inhalation (2.0 to 2.5%) was used for anesthesia. For the ex vivo large-animal lung experiment, all of the tissues were taken from adult Yorkshire Mix Pigs from Research 87 with an average weight of 115 kg. The chronic in vivo large-animal experiments were performed in three Yorkshire pigs (male) weighing 40 to 50 kg, obtained from Parsons, housed in a local animal care facility (Animal Research Facility at Beth Israel Deaconess Medical Center). Anesthesia in pigs was achieved with isoflurane via oral tubes (ventilation frequency, 20/min; tidal volume, 10 ml/kg).

All animal experiments were performed according to the NIH *Guide for the Care and Use of Laboratory Animals* (protocol number 05055 by the Harvard Medical Area Standing Committee on Animals for rat surgery and protocol number 029–2015 by the Institutional Animal Care and Use Committee of the Beth Israel Deaconess Medical Center for pig surgery). All animals were fed standard chow ad libitum. The minimum number of animals per group per readout method was chosenaccordingtotheauthors'experiencetoallowforvalid data[$n = 5$ (in the case of functional rat studies) and 3 (in the case of pig studies)]. All animals were randomly assigned to the different treatment groups. In the case of histology and degradation studies, the investigator conducting the readout method was blinded. In the case of functional studies, the investigators were not blinded.

Subcutaneous implantation in rats

A 1-cm-long incision was created on the dorsum of the rat medially of the spine, and separate subcutaneous pockets were created at the lateral sidesoftheincisions.MeTrosamples($n = 75$;5mm×1mm,disc-shaped) were lyophilized, weighed, measured with digital calipers, and sterilized. The dried sterile hydrogels were then implanted in sterile conditions before anatomical wound closure. At days 7, 28, and 84, MeTro gels with the surrounding tissue were explanted after euthanasia by CO_2 inhalation. Samples were then studied by histological and degradation analysis. Hydrogels used for biodegradation studies were thoroughly washed in distilled water, and excess tissue was carefully removed under a dissection microscope. The samples were then lyophilized, weighed, and measured with digital calipers. In vivo degradation was measured on the basis of the changes in weights and sizes of the samples before and after implantation (62, 63).

Burst pressure tests of sealed rat lung and aorta

The burst pressure of the MeTro gel ($n = 4$) and Evicel ($n = 3$) was tested on sealed rat lungs and arteries. Under sterile conditions, a right-lateral thoracotomy or a median laparotomy was performed to expose the lung or aorta, and placement of retractors maintained surgical access. A 2-mm cut was made using a no. 11 blade scalpel. After removing the hemorrhaged blood, and short proximal ligature in the case of the artery bleeding model, the wound

was dried by filter paper followed by local administration of the MeTro solution (20 μl) and subsequent photo-crosslinking with UV light for 30 s (OmniCure S2000). The thorax or the abdomen was anatomically closed, and in the case of the lung model, de-airing was achieved by using a thorax drainage system. The animals recovered from anesthesia under ventilation. Four days after surgery, the lung or aortic tissue in the former defect area was explanted. Burst pressure tests were performed for both tissues and compared to the corresponding healthy tissues, as well as to Evicel-sealed tissue in the case of the lung model. Figure 5A (i) displays the technical setting for burst pressure measurements. The coherence at the interface of MeTro and tissue (MeTro/lung and MeTro/artery) was studied by SEM and H&E staining. At least five samples were tested for each condition.

Ex vivo burst pressure tests of sealed porcine lung

The burst pressure of the MeTro gel ($n = 5$), Evicel ($n = 3$), Progel ($n = 5$), and surgical sutures ($n = 3$) was determined using an ex vivo porcine lung model. The lungs were kept in a cold room at 4°C before testing. To reduce necrotic variation in the tissue samples, lungs were excluded from the experiment 12 hours after resection. An open-top 56-liter tub was used as a reservoir. The tub was filled with PBS at 37°C. Preceding the burst pressure tests, all lungs were analyzed for defects. A lung was manually connected to a portable volume ventilator (LP3 Portable Ventilator; Life Products Inc.) and expanded at a constant positive pressure of 10 cmH$_2$O for 10 min to ensure that there was no defect. Lobes that presented air leaks, or failed to appropriately inflate, were excluded before the test. A standardized superficial wound of 1 cm was created on the lobe by adhering a 1-cm-diameter cylindrical mold to the visceral pleura of the lung using an ethyl 2-cyanoacrylate glue (Sigma-Aldrich) followed by removal of the visceral pleural layer with a scalpel. The MeTro solution was then administered on the wound and photocrosslinked by irradiation with UV light for 30 s (OmniCure S2000). The burst pressure of the hydrogel was determined by constantly increasing the ventilation pressure and recorded at the first appearance of air bubbles rising from the broken seal.

Lung leakage sealing capacity in large animals

After a right lateral thoracotomy, a standard incision (15 mm × 15 mm × 1 mm) was generated on the lung with a scalpel. All the tested pigs showed air bubbles ($d > 2$ mm) and blood flow from the defect in an immersion test with intrapleural warm PBS. A 20% (w/v) MeTro solution with high degree of methacryloyl substitution was used in these experiments. The MeTro solution (500 μl) was applied on the wound and photocrosslinked via irradiation with UV light for 60 s. The sealed wound was submerged in warm PBS to test for initial leakage. The thorax was closed under de-airing of the pleura using a thorax drainage system. The animals recovered from anesthesia under ventilation. Freedom from pneumothorax was checked by pleural ultrasound imaging on postoperative days 7 and 14 by an Acuson Sequoia C512 sonography system (Siemens Healthcare). At postoperative day 14, the pigs were humanely euthanized, and the wound region sealed by MeTro was excised and further processed for histology analysis.

Histology and immunohistology

MeTro samples with surrounding tissue (5-μm cryosection slides) were used for histological analysis. The sections were fixed with paraformaldehyde and stained with H&E and Masson's trichrome, as well as immunohistological techniques, as previously reported (64). Anti-CD68, anti-CD3 (Abcam), and anti–macrophage-2 (Mac2) (Cedarlane) primary antibodies with Alexa Fluor–conjugated (Invitrogen) secondary antibodies were applied. The sections were further stained by Vecta-shield antifade mounting medium with DAPI (Vector Laboratories). The histology slides ($n = 3$ sections per sample) were examined ($n = 3$ pictures per section) using an Axio Observer microscope (Zeiss).

Statistical analysis

Statistical analysis was performed using one- or two-way ANOVA methods, followed by Tukey's multiple comparisons test. $P < 0.05$ was defined as significant for all statistical tests. Data are means ± SD. All statistical analysis and graphing were performed with GraphPad Prism version 6 software.

Supplementary Material

Refer to Web version on PubMed Central for supplementary material.

Acknowledgments

Data and materials availability:

All data are included in this paper or the Supplementary Materials. Tropoelastin is available from Elastagen Pty Ltd. under a material transfer agreement with the University. Additional materials can be obtained by request to N.A. and A.K.

REFERENCES AND NOTES

1. Annabi N, Tamayol A, Shin SR, Ghaemmaghami AM, Peppas NA, Khademhosseini A, Surgical materials: Current challenges and nano-enabled solutions. Nano Today 9, 574–589 (2014). [PubMed: 25530795]

2. Smith TO, Sexton D, Mann C, Donell S, Sutures versus staples for skin closure in orthopaedic surgery: Meta-analysis. BMJ 340, c1199 (2010). [PubMed: 20234041]

3. Sanders L, Nagatomi J, Clinical applications of surgical adhesives and sealants. Crit. Rev. Biomed. Eng. 42, 271–292 (2014). [PubMed: 25597240]

4. Lins RD, Gomes RC, Santos KS, Silva PV, Silva RT, Ramos IA, Use of cyanoacrylate in the coaptation of edges of surgical wounds. An. Bras. Dermatol. 87, 871–876 (2012). [PubMed: 23197206]

5. Burdick JA, Murphy WL, Moving from static to dynamic complexity in hydrogel design. Nat. Commun. 3, 1269 (2012). [PubMed: 23232399]

6. Spotnitz WD, Hemostats, sealants, and adhesives: A practical guide for the surgeon. Am. Surg. 78, 1305–1321 (2012). [PubMed: 23265118]

7. Scognamiglio F, Travan A, Rustighi I, Tarchi P, Palmisano S, Marsich E, Borgogna M, Donati I, de Manzini N, Paoletti S, Adhesive and sealant interfaces for general surgery applications. J. Biomed. Mater. Res. B Appl. Biomater. 104, 626–639 (2016). [PubMed: 25891348]

8. Ferreira P, Pereira R, Coelho JFJ, Silva AFM, Gil MH, Modification of the biopolymer castor oil with free isocyanate groups to be applied as bioadhesive. Int. J. Radiat. Biol. Relat. Stud. Phys. Chem. Med. 40, 144–152 (2007).

9. Oliveira CL, dos Santos CHM, Bezerra FMM, Bezerra MM, de Lima Rodrigues L, Utilization of cyanoacrylates adhesives in skin suture. Rev. Bras. Cir. Plást. 25, 573–576 (2010).

10. Ernsting J, Nicholson AN, Rainford DJ, Aviation Medicine (Butterworth-Heinemann, ed. 3,1999).

11. Levental I, Georgesa PC, Janmey PA, Soft biological materials and their impact on cell function. Soft Matter 3, 299–306 (2007). [PubMed: 32900146]

12. Carver W, Goldsmith EC, Regulation of tissue fibrosis by the biomechanical environment. BioMed Res. Int. 2013, 101979 (2013).

13. Mann S, Craig MW, Gould BA, Melville DI, Raftery EB, Coital blood pressure in hypertensives. Cephalgia, syncope, and the effects of beta-blockade. Br. Heart J. 47, 84–89 (1982). [PubMed: 6119996]

14. Belboul A, Dernevik L, O.m, Skrbic B, Rådberg G, Roberts D, The effect of autologous fibrin sealant (Vivostat®) on morbidity after pulmonary lobectomy: A prospective randomised, blinded study. Eur. J. Cardiothorac. Surg. 26, 1187–1191 (2004). [PubMed: 15541982]

15. Cerfolio RJ, Bass CS, Pask AH, Katholi CR, Predictors and treatment of persistent air leaks. Ann. Thorac. Surg. 73, 1727–1731 (2002). [PubMed: 12078760]

16. Kirsh MM, Rotman H, Behrendt DM, Orringer MB, Sloan H, Complications of pulmonary resection. Ann. Thorac. Surg. 20, 215–236 (1975). [PubMed: 1099996]

17. D'Andrilli A, Andreetti C, Ibrahim M, Ciccone AM, Venuta F, Mansmann U, Rendina EA, A prospective randomized study to assess the efficacy of a surgical sealant to treat air leaks in lung surgery. Eur. J. Cardiothorac. Surg. 35, 817–821 (2009). [PubMed: 19269837]

18. Bertolaccini L, Lyberis P, Manno E, Lung sealant and morbidity after pleural decortication: A prospective randomized, blinded study. J. Cardiothorac. Surg. 5, 45 (2010). [PubMed: 20509919]

19. Brunelli A, Monteverde M, Borri A, Salati M, Marasco RD, Fianchini A, Predictors of prolonged air leak after pulmonary lobectomy. Ann. Thorac. Surg. 77, 1205–1210 (2004). [PubMed: 15063235]

20. Thistlethwaite PA, Luketich JD, Ferson PF, Keenan RJ, Jamieson SW, Ablation of persistent air leaks after thoracic procedures with fibrin sealant. Ann. Thorac. Surg. 67, 575–577 (1999). [PubMed: 10197706]

21. Izbicki JR, Kreusser T, Meier M, Prenzel KL, Knoefel WT, Passlick B, Kuntz G, Schiele U, Thetter O, Fibrin-glue-coated collagen fleece in lung surgery—Experimental comparison with infrared coagulation and clinical experience. Thorac. Cardiovasc. Surg. 42, 306–309 (1994). [PubMed: 7863495]

22. Wong K, Goldstraw P, Effect of fibrin glue in the reduction of postthoracotomy alveolar air leak. Ann. Thorac. Surg. 64, 979–981 (1997). [PubMed: 9354513]

23. Mehdizadeh M, Yang J, Design strategies and applications of tissue bioadhesives. Macromol. Biosci. 13, 271–288 (2013). [PubMed: 23225776]

24. Sanders L, Stone R, Webb CK, Mefford OT, Nagatomi J, Mechanical characterization of a bi-functional tetronic hydrogel adhesive for soft tissues. J. Biomed. Mater. Res. A 103, 861–868 (2015). [PubMed: 25111445]

25. Ranger WR, Halpin D, Sawhney AS, Lyman M, Locicero J, Pneumostasis of experimental air leaks with a new photopolymerized synthetic tissue sealant. Am. Surg. 63, 788–795 (1997). [PubMed: 9290523]

26. Allen MS, Wood DE, Hawkinson RW, Harpole DH, McKenna RJ, Walsh GL, Vallieres E, Miller DL, Nichols FC, Smythe WR, Davis RD; 3M Surgical Sealant Study Group, Prospective

randomized study evaluating a biodegradable polymeric sealant for sealing intraoperative air leaks that occur during pulmonary resection. Ann. Thorac. Surg. 77, 1792–1801 (2004). [PubMed: 15111188]

27. Wain JC, Kaiser LR, Johnstone DW, Yang SC, Wright CD, Friedberg JS, Feins RH, Heitmiller RF, Mathisen DJ, Selwyn MR, Trial of a novel synthetic sealant in preventing air leaks after lung resection. Ann. Thorac. Surg. 71, 1623–1629 (2001). [PubMed: 11383811]

28. Torchiana DF, Polyethylene glycol based synthetic sealants: Potential uses in cardiac surgery. J. Card. Surg. 18, 504–506 (2003). [PubMed: 14992100]

29. Fuller C, Reduction of intraoperative air leaks with Progel in pulmonary resection: A comprehensive review. J. Cardiothorac. Surg. 8, 90 (2013). [PubMed: 23590942]

30. Kobayashi H, Sekine T, Nakamura T, Shimizu Y, In vivo evaluation of a new sealant material on a rat lung air leak model. J. Biomed. Mater. Res. 58, 658–665 (2001). [PubMed: 11745518]

31. Lang N, Pereira MJ, Lee Y, Friehs I, Vasilyev NV, Feins EN, Ablasser K, O'Cearbhaill ED, Xu C, Fabozzo A, Padera R, Wasserman S, Freudenthal F, Ferreira LS, Langer R, Karp JM, del Nido PJ, A blood-resistant surgical glue for minimally invasive repair of vessels and heart defects. Sci. Transl. Med. 6, 218ra6 (2014).

32. Annabi N, Mithieux SM, Zorlutuna P, Camci-Unal G, Weiss AS, Khademhosseini A, Engineered cell-laden human protein-based elastomer. Biomaterials 34, 5496–5505 (2013). [PubMed: 23639533]

33. Annabi N, Tsang K, Mitheux SM, Nikkhah M, Ameri A, Khademhosseini A, Weiss AS, Highly elastic micropatterned hydrogel for engineering functional cardiac tissue. Adv. Funct. Mater. 23, 4950–4959 (2013).

34. Annabi N, Rana D, Shirzaei SE, Portillo-Lara R, Gifford JL, Fares MM, Mithieux SM, Weiss AS, Engineering a sprayable and elastic hydrogel adhesive with antimicrobial properties for wound healing. Biomaterials 139, 229–243 (2017). [PubMed: 28579065]

35. Annabi N, Shin SR, Tamayol A, Miscuglio M, Bakooshli MA, Assmann A, Mostafalu P, Sun J-Y, Mithieux S, Cheung L, Tang X, Weiss AS, Khademhosseini A, Highly elastic and conductive human-based protein hybrid hydrogels. Adv. Mater. 28, 40–49 (2016). [PubMed: 26551969]

36. Mithieux SM, Rasko JEJ, Weiss AS, Synthetic elastin hydrogels derived from massive elastic assemblies of self-organized human protein monomers. Biomaterials 25, 4921–4927 (2004). [PubMed: 15109852]

37. Mithieux SM, Tu Y, Korkmaz E, Braet F, Weiss AS, In situ polymerization of tropoelastin in the absence of chemical cross-linking. Biomaterials 30, 431–435 (2009). [PubMed: 18996590]

38. Baldock C, Oberhauser AF, Ma L, Lammie D, Siegler V, Mithieux SM, Tu Y, Chow JYH, Suleman F, Malfois M, Rogers S, Guo L, Irving TC, Wess TJ, Weiss AS, Shape of tropoelastin, the highly extensible protein that controls human tissue elasticity. Proc. Natl. Acad. Sci. U.S.A. 108, 4322–4327 (2011). [PubMed: 21368178]

39. Elvin CM, Vuocolo T, Brownlee AG, Sando L, Huson MG, Liyou NE, Stockwell PR, Lyons RE, Kim M, Edwards GA, Johnson G, McFarland GA, Ramshaw JA, Werkmeister JA, A highly elastic tissue sealant based on photopolymerised gelatin. Biomaterials 31, 8323–8331 (2010). [PubMed: 20674967]

40. Vuocolo T, Haddad R, Edwards GA, Lyons RE, Liyou NE, Werkmeister JA, Ramshaw JA, Elvin CM, A highly elastic and adhesive gelatin tissue sealant for gastrointestinal surgery and colon anastomosis. J. Gastrointest. Surg. 16, 744–752 (2012). [PubMed: 22081305]

41. Annabi N, Tamayol A, Uquillas JA, Akbari M, Bertassoni LE, Cha C, Camci-Unal G, Dokmeci MR, Peppas NA, Khademhosseini A, 25th anniversary article: Rational design and applications of hydrogels in regenerative medicine. Adv. Mater. 26, 85–124 (2014). [PubMed: 24741694]

42. Annabi N, Nichol JW, Zhong X, Ji C, Koshy S, Khademhosseini A, Dehghani F, Controlling the porosity and microarchitecture of hydrogels for tissue engineering. Tissue Eng. Part B Rev. 16, 371–383 (2010). [PubMed: 20121414]

43. Ahmed EM, Hydrogel: Preparation, characterization, and applications: A review. J. Adv. Res. 6, 105–121 (2015). [PubMed: 25750745]

44. Marini JJ, Recruitment by sustained inflation: Time for a change. Intensive Care Med. 37, 1572–1574 (2011). [PubMed: 21858521]

45. Urry DW, Parker TM, Reid MC, Gowda DC, Biocompatibility of the bioelastic materials, poly(GVGVP) and its g-irradiation cross-linked matrix: Summary of generic biological test results. J. Bioact. Compat. Polym. 6, 263 (1991).

46. Tu Y, Weiss AS, Transient tropoelastin nanoparticles are early-stage intermediates in the coacervation of human tropoelastin whose aggregation is facilitated by heparan sulfate and heparin decasaccharides. Matrix Biol. 29, 152–159 (2010). [PubMed: 19895887]

47. Taddese S, Weiss AS, Jahreis G, Neubert RHH, Schmelzer CEH, In vitro degradation of human tropoelastin by MMP-12 and the generation of matrikines from domain 24. Matrix Biol. 28, 84–91 (2009). [PubMed: 19144321]

48. Ennis BW, Matrisian LM, Matrix degrading metalloproteinases. J. Neurooncol 18, 105–109 (1993).

49. Morgunova E, Tuuttila A, Bergmann U, Isupov M, Lindqvist Y, Schneider G, Tryggvason K, Structure of human pro-matrix metalloproteinase-2: Activation mechanism revealed. Science 284, 1667–1670 (1999). [PubMed: 10356396]

50. Spotnitz WD, Fibrin sealant: The only approved hemostat, sealant, and adhesive-a laboratory and clinical perspective. ISRN Surg. 2014, 203943 (2014).

51. Annabi N, Yue K, Tamayol A, Khademhosseini A, Elastic sealants for surgical applications. Eur. J. Pharm. Biopharm. 95, 27–39 (2015). [PubMed: 26079524]

52. Duarte AP, Coelho JF, Bordado JC, Cidade MT, Gil MH, Surgical adhesives: Systematic review of the main types and development forecast. Prog. Polym. Sci. 37, 1031–1050 (2012).

53. Bouten PJM, Zonjee M, Bender J, Yauw STK, van Goor H, van Hest JCM, Hoogenboom R, The chemistry of tissue adhesive materials. Prog. Polym. Sci. 39, 1375–1405 (2014).

54. Singer AJ, Quinn JV, Hollander JE, The cyanoacrylate topical skin adhesives. Am. J. Emerg. Med. 26, 490–496 (2008). [PubMed: 18410821]

55. Singer AJ, Thode HC Jr., A review of the literature on octylcyanoacrylate tissue adhesive. Am. J. Surg. 187, 238–248 (2004). [PubMed: 14769312]

56. Montanaro L, Arciola CR, Cenni E, Ciapetti G, Savioli F, Filippini F, Barsanti LA, Cytotoxicity, blood compatibility and antimicrobial activity of two cyanoacrylate glues for surgical use. Biomaterials 22, 59–66 (2001). [PubMed: 11085384]

57. Sierra DH, Eberhardt AW, Lemons JE, Failure characteristics of multiple-component fibrin-based adhesives. J. Biomed. Mater. Res. 59, 1–11 (2002). [PubMed: 11745531]

58. Ikada Y, Absorbable hydrogels for medical use, in Gels Handbook Y, Kajiwara K, Fushimi T, Irasa O, Hirokawa Y, Matsunaga T, Shimomura T, Wang L, Ishida H, Eds. (Academic Press, 2000).

59. Behrens AM, Lee NG, Casey BJ, Srinivasan P, Sikorski MJ, Daristotle JL, Sandler AD, Kofinas P, Biodegradable-polymer-blend-based surgical sealant with body-temperature-mediated adhesion. Adv. Mater. 27, 8056–8061 (2015). [PubMed: 26554545]

60. Yeo GC, Keeley FW, Weiss AS, Coacervation of tropoelastin. Adv. Colloid Interface Sci. 167, 94–103 (2011). [PubMed: 21081222]

61. Dehghani F, Annabi N, Valtchev P, Mithieux SM, Weiss AS, Kazarian SG, Tay FH, Effect of dense gas CO_2 on the coacervation of elastin. Biomacromolecules 9, 1100–1105 (2008). [PubMed: 18363358]

62. Zhang Y-N, Avery RK, Vallmajo-Martin Q, Assmann A, Vegh A, Memic A, Olsen BD, Annabi N, Khademhosseini A, A highly elastic and rapidly crosslinkable elastin-like polypeptide-based hydrogel for biomedical applications. Adv. Funct. Mater. 25, 4814–4826 (2015). [PubMed: 26523134]

63. Nunamaker EA, Purcell EK, Kipke DR, In vivo stability and biocompatibility of implanted calcium alginate disks. J. Biomed. Mater. Res. A 83, 1128–1137 (2007). [PubMed: 17595019]

64. Assmann A, Zwirnmann K, Heidelberg F, Schiffer F, Horstkötter K, Munakata H, Gremse F, Barth M, Lichtenberg A, Akhyari P, The degeneration of biological cardiovascular prostheses under pro-calcific metabolic conditions in a small animal model. Biomaterials 35, 7416–7428 (2014). [PubMed: 24917029]
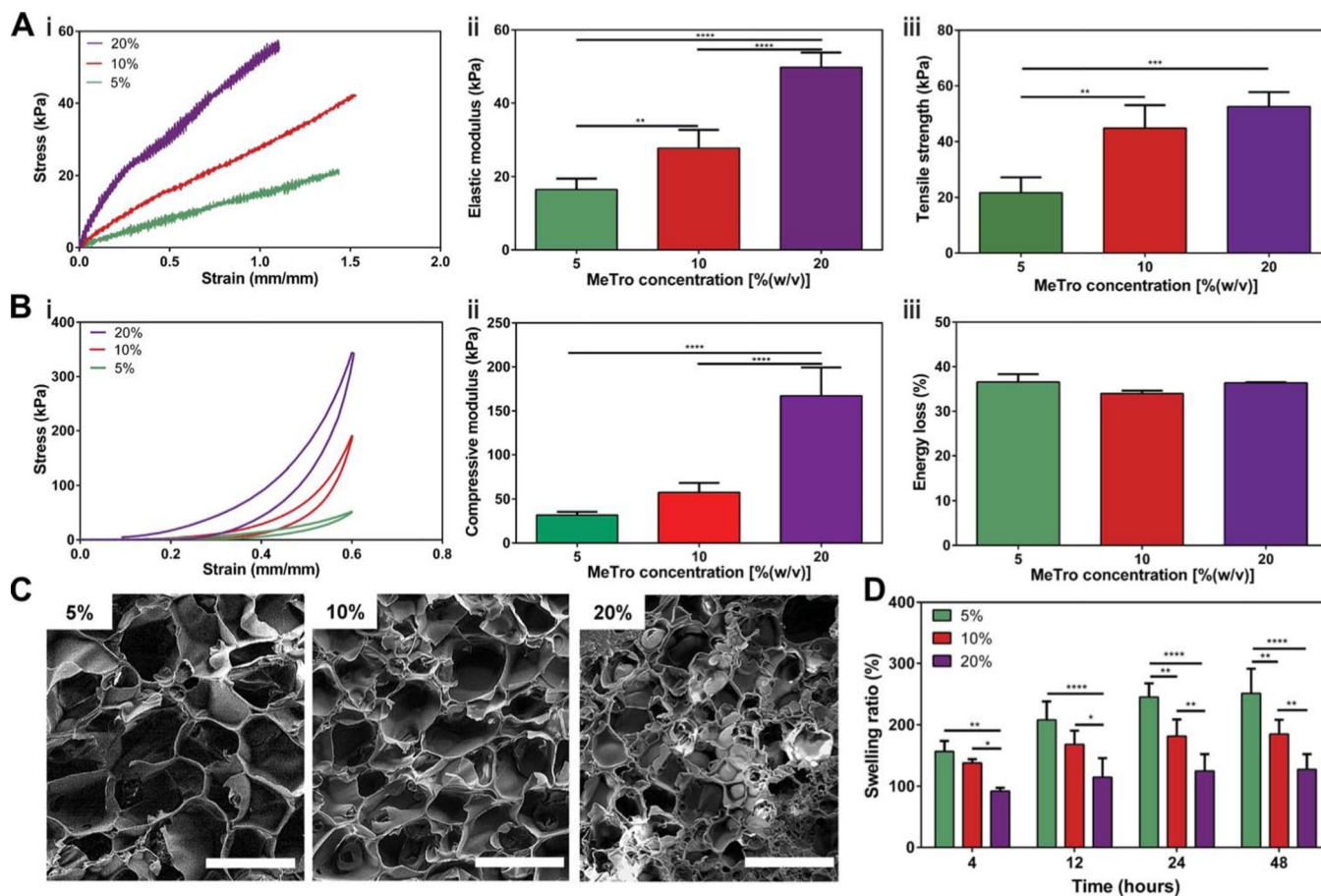
Fig. 1. Physical characterizations of the MeTro sealant.
(**A**) Tensile tests on the MeTro hydrogel produced by using different MeTro concentrations with medium degree of methacryloyl substitution (76%) (n 3). (i) Representative tensile strain-stress curves, (ii) elastic modulus, and (iii) ultimate tensile strength. (**B**) Compression tests on the MeTro hydrogel produced at different MeTro concentrations with medium degree of methacryloyl substitution ($n = 3$). (i) Representative compression strain-stress curves, (ii) compressive modulus, and (iii) energy loss. (**C**) Representative SEM images of the MeTro hydrogel synthesized by (i) 5%, (ii) 10%, and (iii) 20% (w/v) MeTro concentrations at medium degree of methacryloyl substitution (scale bars, 100 μm). (**D**) Swelling ratios of the MeTro hydrogel in PBS at 37°C, depending on different MeTro concentrations with the medium methacryloyl substitution over 48 hours ($n = 4$). Data are means ± SD. P values were determined by one-way analysis of variance (ANOVA) followed by Tukey's multiple comparisons test for (A) and (B), and two-way ANOVA for (D) (*$P < 0.05$, **$P < 0.01$, ***$P < 0.001$, ****$P < 0.0001$).
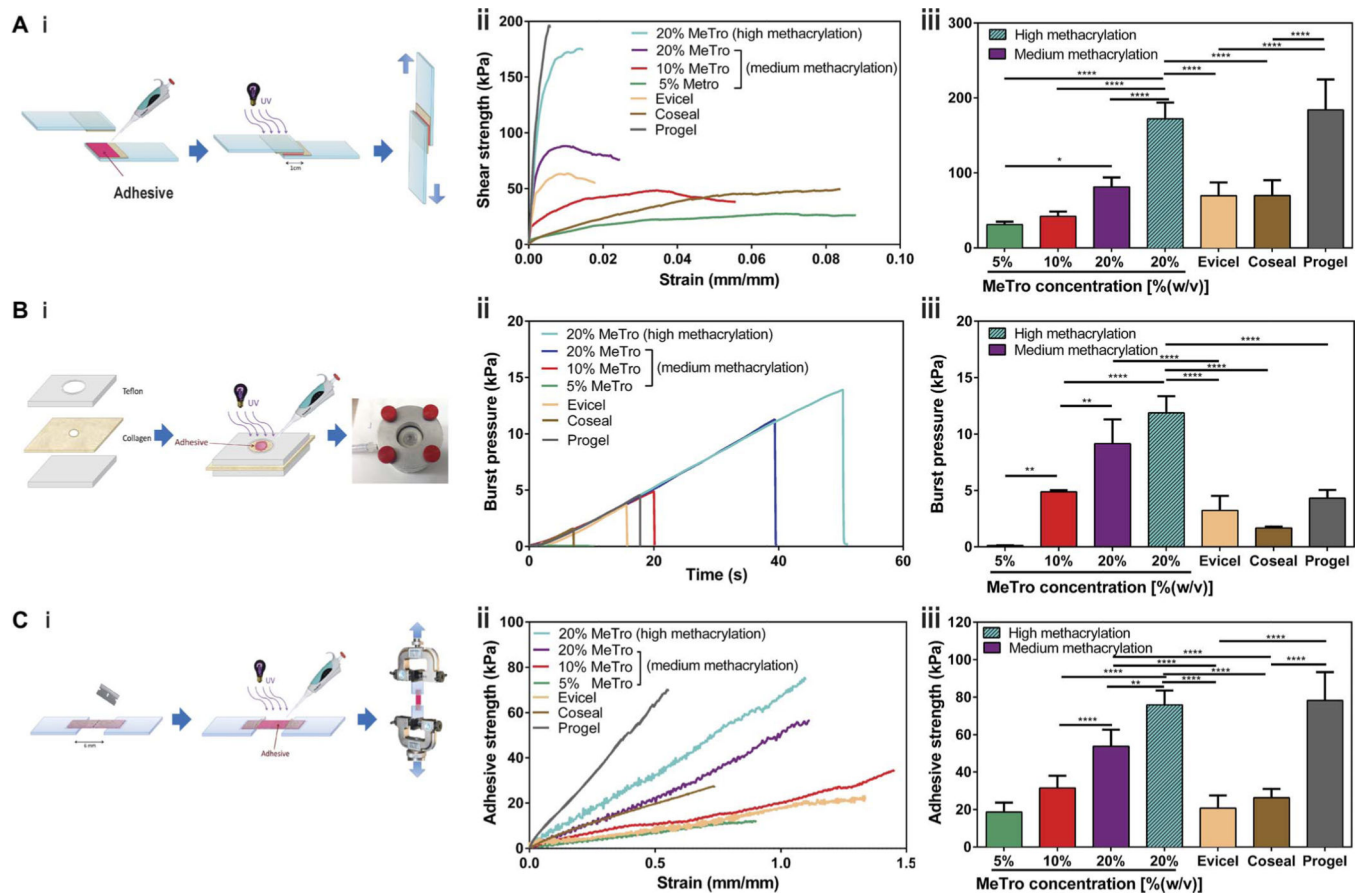
Fig. 2. In vitro sealing properties of the MeTro sealant.

(**A**) Standard lap shear test to determine the shear strength of MeTro sealants (*n* ≥ 4) with different formulations and several commercially available sealants: Evicel (*n* = 5), Coseal (*n* = 3), and Progel (*n* = 4). (i) Schematic of the modified standard test method for shear test (ASTM F2255–05), (ii) representative strain-stress curves for lap shear tests, and (iii) average shear strength of MeTro sealants produced with varying MeTro concentrations and degree of methacryloyl substitution, and commercially available sealants including Evicel, Coseal, and Progel. (**B**) Standard burst pressure test to evaluate the burst pressure of the MeTro sealant (*n* ≥ 4) with different formulations [except 5% Metro (*n* = 2)] and several commercially available sealants: Evicel (*n* = 4), Coseal (*n* = 3), and Progel (*n* = 5). (i) Schematic of the modified standard test method for the burst pressure (ASTM F2392–04), (ii) representative strain-stress curves for burst pressure test, and (iii) average burst pressure of the MeTro sealants with variable MeTro concentrations and degree of methacryloyl substitution, and commercially available sealants. (**C**) Standard wound closure using porcine skin as the biological substrate to test the adhesion strength of the MeTro sealant (*n* ≥ 4) with different formulations and commercially available sealants: Evicel (*n* = 5), Coseal (*n* = 3), and Progel (*n* = 3). (i) Schematic of the modified standard test method for adhesion strength (ASTM F2458–05), (ii) representative strain-stress curves for wound closure test, and (iii) average adhesive strength of MeTro sealants produced with variable MeTro concentrations and degree of methacryloyl substitution, and their comparison with
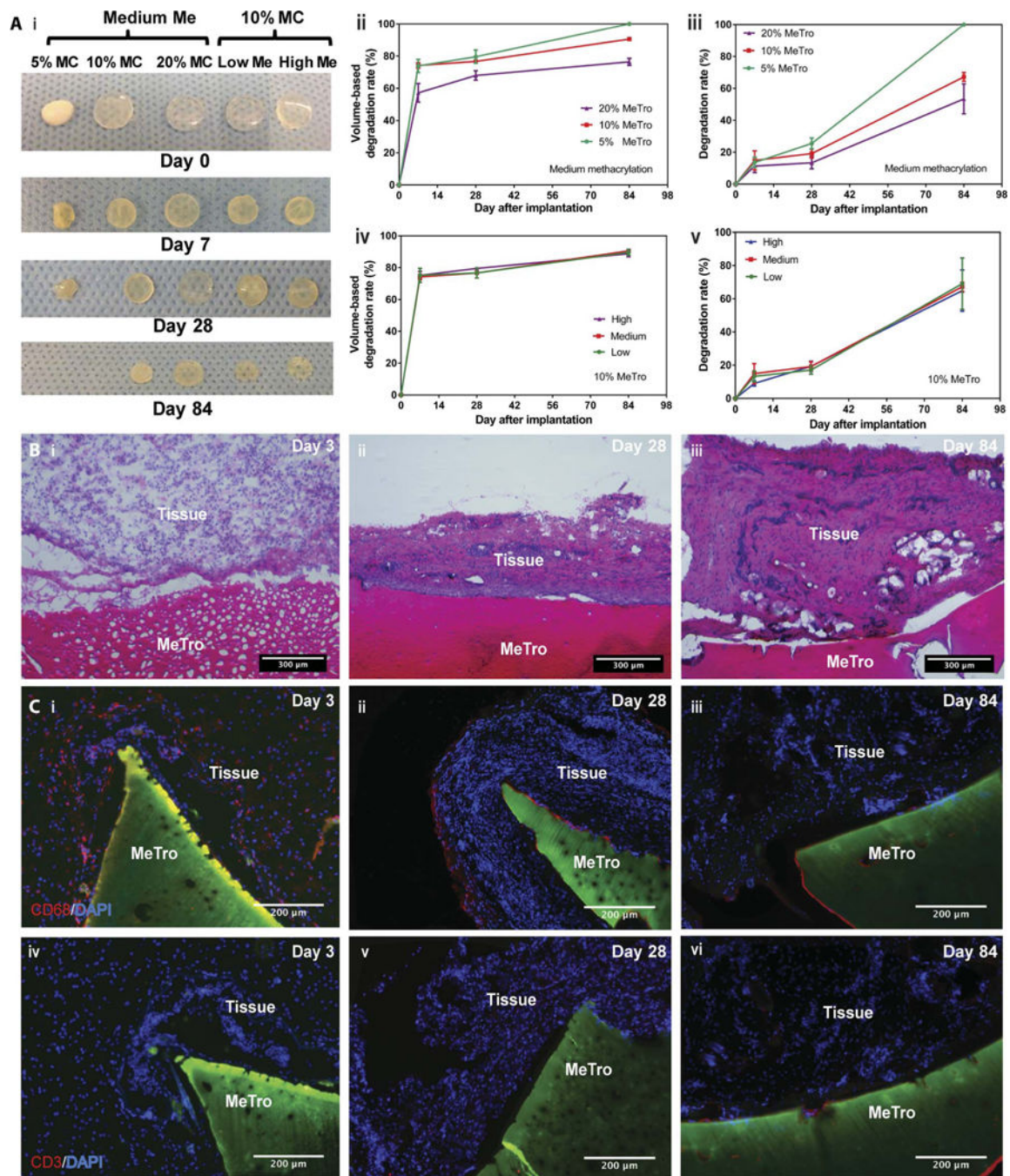
commercially available sealants. Data are means ± SD. *P* values were determined by one-way ANOVA followed by Tukey's multiple comparisons test (*$P < 0.05$, **$P < 0.01$, ****$P < 0.0001$).

Fig. 3. In vivo biocompatibility and degradation of the MeTro sealant using a rat subcutaneous model.

(**A**) Evaluation of the in vivo degradation of MeTro sealants on days 0, 7, 28, and 84 of implantation ($n = 4$). (i) Representative images of the MeTro hydrogel implants with different extents of methacryloyl substitution (Me) and MeTro concentrations (MC). In vivo MeTro degradation based on volume loss of the implant for (ii) varying MeTro concentrations with medium methacryloyl substitution and (iv) varying extents of methacryloyl substitution at 10% (w/v) MeTro concentration. In vivo MeTro degradation

based on weight loss of the implant for (iii) variable MeTro concentration with medium methacryloyl substitution and (v) variable degree of methacryloyl substitution at 10% (w/v) MeTro concentration. The in vivo degradation profile of MeTro hydrogels shows significant volume loss by day 7 and almost constant weight loss afterward until day 84. (**B**) Histology images of MeTro with the surrounding tissue stained with H&E after (i) 3 days, (ii) 28 days, and (iii) 84 days of implantation in subcutaneous tissue of a rat using 20% MeTroconcentration and medium methacryloyl substitution (scale bars, 300 μm). H&E reveals insignificant amount of inflammatory cells. (**C**) Immunostaining of subcutaneously implanted MeTro hydrogels showing macrophage (CD68) only at (i) day 3 but disappeared at days (ii) 28 and (iii) 84, and resulting in no local lymphocyte infiltration (CD3) at days (iv) 3, (v) 28, and (vi) 84 (scale bars, 200 μm). Green color in (C) and (D) represents the autofluorescent MeTro gel, red color represents the lymphocytes, and blue color represents the nuclei (DAPI).
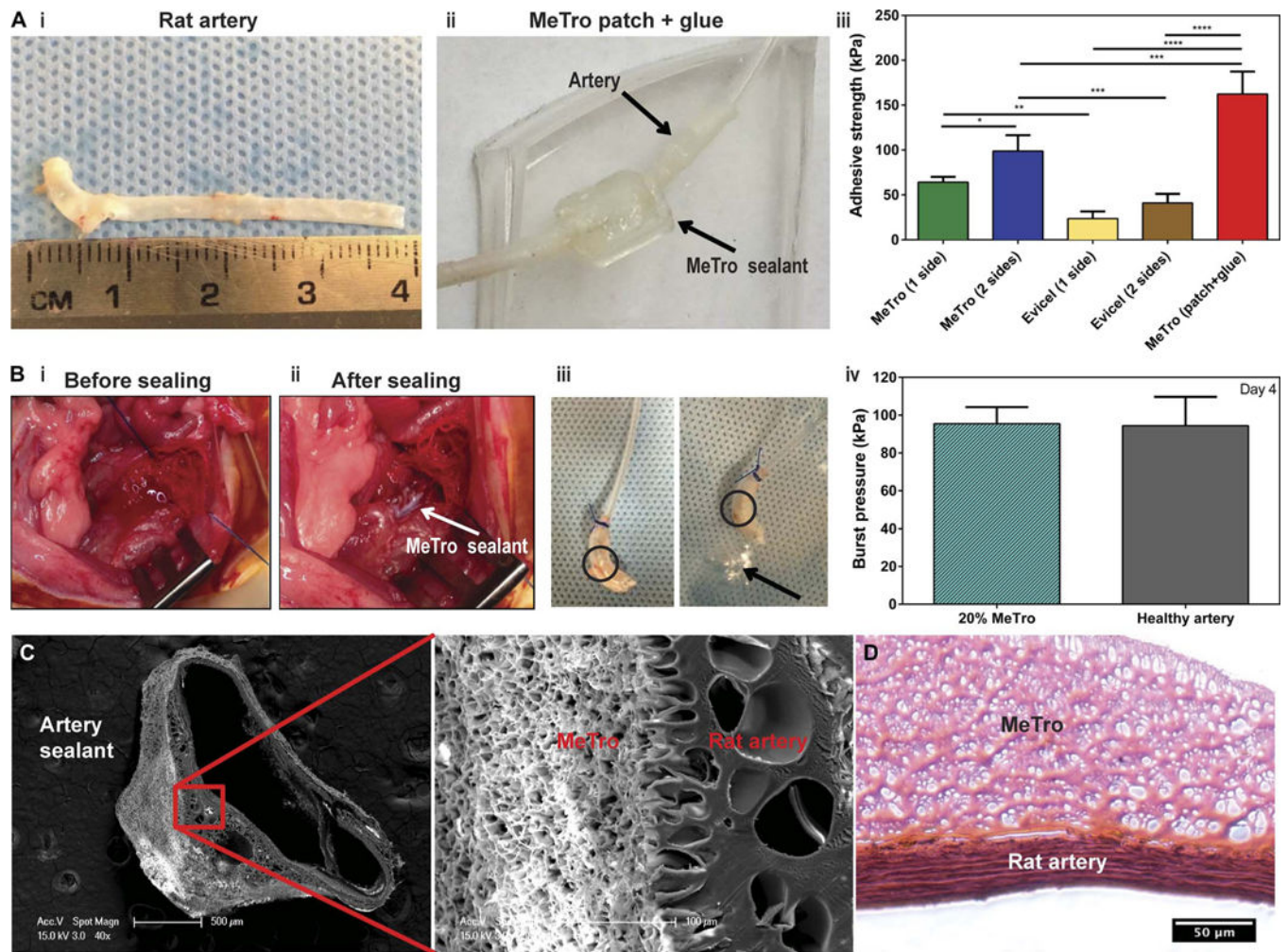
Fig. 4. Ex vivo and in vivo function of the MeTro sealant using rat incision model of arteries.
(**A**) Ex vivo wound closure test using explanted rat aorta as a biological substrate for
tissue adhesion. (i) An explanted aorta from a rat (about 4 cm in length). (ii) A patch
generated using the MeTro hydrogel and wrapped the artery tube segments. The connecting
anastomosis points were further glued with MeTro. Arrows present the rat artery and MeTro
sealant. (iii) Adhesive strength of the MeTro sealant applied on one side ($n = 4$) and
both sides ($n = 3$) of the artery in comparison with Evicel applied on one side ($n = 4$)
and both sides ($n = 4$). The MeTro patch ($n = 2$) further improved the adhesive strength.
(**B**) In vivo tests on rat arteries sealed by MeTro ($n = 3$). Operative sites (i) before and
(ii) after sealing. White arrow presents the MeTro sealant on the artery. (iii) Image of
a sealed artery pressurized with air, demonstrating that MeTro could adhere to the outer
arterial surface and seal the incision, but the artery burst in another area. Circles present
the MeTro seals. Arrow indicates bubbles from the burst point on the artery instead of
the MeTro sealing site. (iv) Burst pressure values of artery sealed by MeTro with 20%
concentration and high methacryloyl substitution after 4 days compared to a healthy artery
as a control. Representative SEM (**C**) and H&E-stained (**D**) images from the interface
between the explanted rat artery and the MeTro sealant. Tight interfaces between the MeTro

hydrogel and the tissues indicate strong bonding and interlocking at the interfaces. Data are means ± SD. P values were determined by one-way ANOVA followed by Tukey's multiple comparisons test for (A) and (B) (*$P < 0.05$, **$P < 0.01$, ***$P < 0.001$, ****$P < 0.0001$).
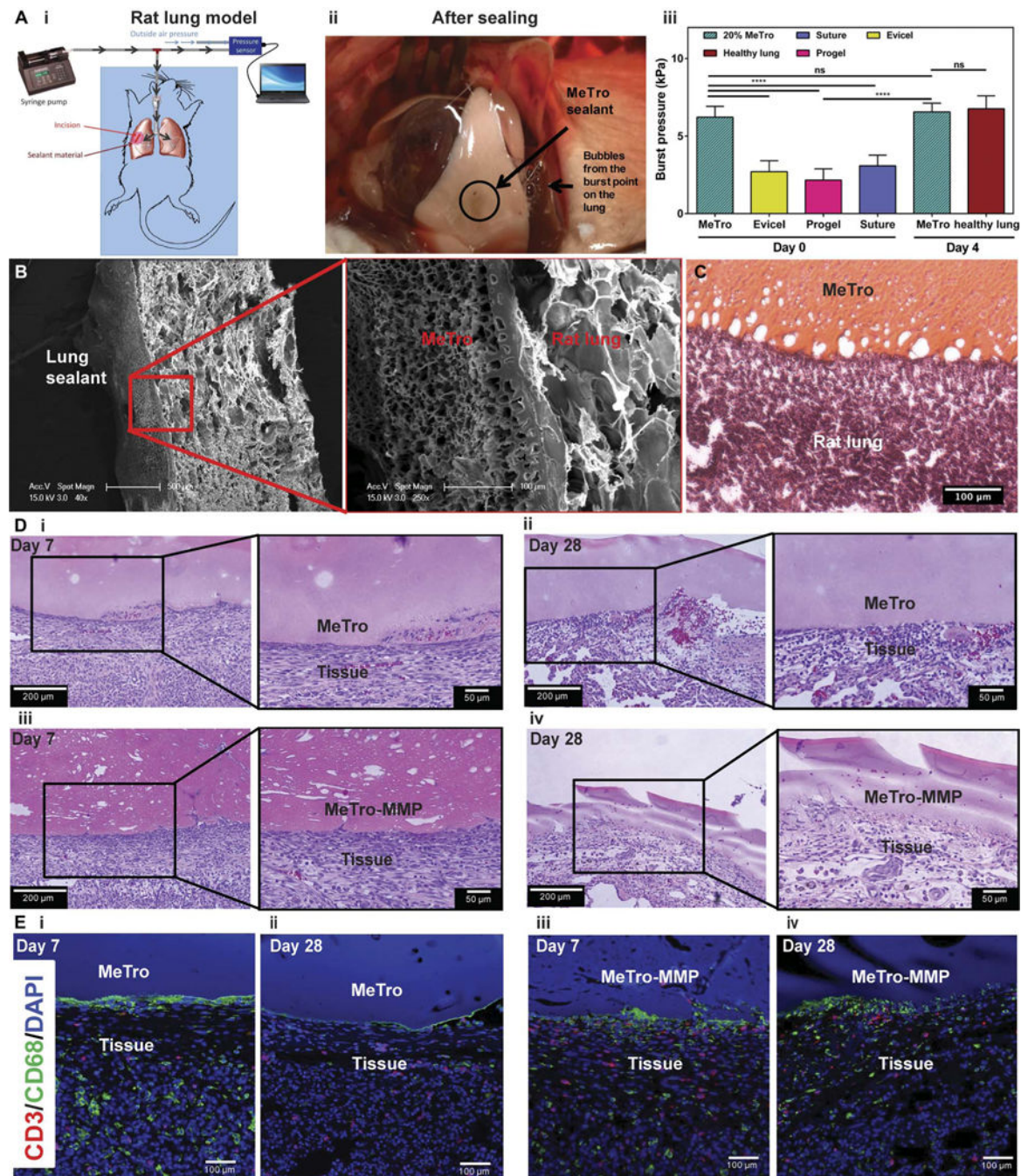
Fig. 5. In vivo function of MeTro sealants using rat incision model of lungs.
(**A**) In vivo tests on rat lungs sealed by MeTro. (i) Schematic diagram showing the experimental setup. (ii) Image of the sealed lung pressurized with air, demonstrating that MeTro could adhere to the lung surface and seal the incision, but the lung tissue burst from other areas (the source of the bubbles) when pressures of >5.5 kPa were applied. (iii) Burst pressure values for lungs sealed with the MeTro sealant on day 0 ($n = 4$) and day 4 ($n = 3$) as compared to lungs sealed by Evicel ($n = 3$), Progel ($n = 6$), and suture only ($n = 6$) as well as healthy lung ($n = 3$) on day 0. Representative (**B**) SEM and (**C**) H&E-stained images

from the interface between the explanted rat lung and the MeTro sealant. Tight interfaces between the MeTro hydrogel and the tissues indicate strong bonding and interlocking at the interfaces. (**D**) H&E staining of MeTro sections at days (i) 7 and (ii) 28 and MeTro-MMP sections at days (iii) 7 and (iv) 28 after sealing. (**E**) Fluorescent immunohistochemical analysis of the MeTro and MeTro-MMP sealants, showing no significant local lymphocyte infiltration (CD3) at days (i) 7 and (ii) 28 for MeTro samples and at days (iii) 7 and (iv) 28 for MeTro-MMP samples. Also, the images exhibit remarkable macrophage (CD68) expression at day 7 (i and iii) but reduced expression at day 28 for MeTro and remained the same for MeTro-MMP samples (ii and iv). Green, red, and blue colors in (E) represent the macrophages, lymphocytes, and cell nuclei (DAPI), respectively. Data are means ± SD. P values were determined by one-way ANOVA followed by Tukey's multiple comparisons test for (A) (**$P < 0.01$, ***$P < 0.001$).
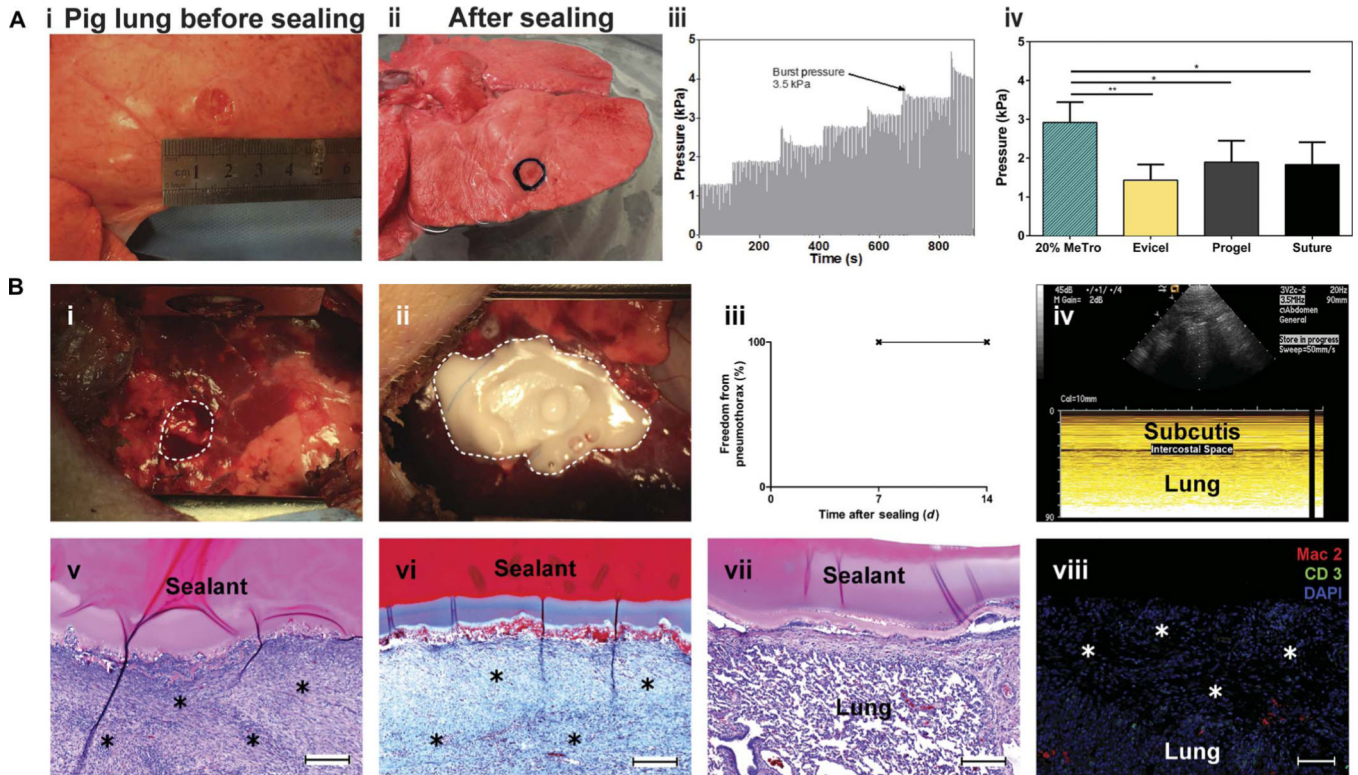
Fig. 6. Ex vivo and in vivo test to evaluate the sealing capability of the MeTro sealant using a porcine lung incision model.
(**A**) Ex vivo porcine lung burst pressure testing. (i) Image from the superficial wound created in deflated lung before sealing, (ii) wound covered with the MeTro sealant, (iii) representative graph depicting the incremental increase in pressure during ventilation, and (iv) average burst pressures for MeTro ($n = 5$), Evicel ($n = 3$), Progel ($n = 5$), and a suture control ($n = 3$). MeTro shows the highest burst pressure. (**B**) In vivo sealing capacity of MeTro using a porcine lung incision model ($n = 3$). (i and ii) A right lung lobe is exposed through a small lateral thoracotomy, and a standardized defect is created [broken line in (B, i)] and sealed by applying and photocrosslinking the MeTro (20% MeTro concentration with high methacryloyl substitution) sealant [broken line in (B, ii)]. (iii and iv) At postoperative days 7 and 14, freedom from pneumothorax was confirmed by sonography, as displayed in a representative ultrasound image at day 14, indicating the absence of any relevant amount of air in the intercostal space. (v) Representative histological sections of the lung leakage site after 14 days revealed sufficient formation of wound healing tissue [asterisks in (v); H&E staining] including a stable collagenous (blue) defect cover [asterisks in (vi); Masson's trichrome staining]. (vii) H&E staining of the attachment of MeTro sealant to noninjured lung tissue around the defect site. (viii) Immunohistological staining of the defect area and the formed wound healing tissue (asterisks) did not show relevant macrophage (Mac2) or lymphocyte (CD3) infiltration. Scale bars, 200 μm (v to vii) and 100 μm (viii). Data are means ± SD (*$P < 0.05$ and **$P < 0.01$).